American Mineralogist, Volume 82, pages 663–671, 1997

Crystal chemistry of forsterite: A first-principles study

RENATA M. WENTZCOVITCH[1] AND LARS STIXRUDE[2]

[1]Department of Chemical Engineering and Materials Sciences, Minnesota Supercomputer Institute, University of Minnesota, Minneapolis, Minnesota 55455, U.S.A.
[2]School of Earth and Atmospheric Sciences, Georgia Institute of Technology, Atlanta, Georgia 30332-0340, U.S.A.

ABSTRACT

We present a first-principles study (local density approximation) of the structural properties of forsterite under pressure. This highly anisotropic magnesium orthosilicate is the most abundant phase of the Earth's upper mantle, and its elastic properties determine the rheology of this region. We perform full structural optimizations and investigate its compressive behavior up to 25 GPa. We obtain a pressure dependence of lattice parameters that agrees well with experiments to 17.2 GPa. We predict that the coordination polyhedra compress essentially isotropically, and we explain the anisotropy of forsterite in terms of the nonuniform distribution of coordination polyhedra having different but nearly uniform compressibilities. In agreement with Brodholt et al. (1996), we do not find theoretical evidence for sudden changes in compression mechanisms in this mineral as had been suggested from experiments. Our results support the hypothesis that such compressive anomalies are caused by solidification of the pressure medium.

INTRODUCTION

The magnesium orthosilicate polymorphs are the dominant mineral phases of the top-most 660 km of Earth's mantle. The low-pressure phase olivine is the major phase of the upper mantle, which represents nearly 20% of the planet's volume. The composition of olivine in the upper mantle consists of ~90% forsterite, the Mg end-member. The properties and behavior of forsterite have been intensively studied because they determine the elasticity and rheology of the asthenospheric mantle and, in turn, plate-tectonic processes. An important observational constraint on the nature of flow in the sub-lithospheric mantle comes from seismological observations of anisotropy, which originate in the intrinsic elastic anisotropy of olivine. Moreover, the pressure-induced transformation of forsterite to wadsleyite under equilibrium conditions is largely responsible for the seismic discontinuity observed at depths of 400 km within the Earth. Lower temperatures suppress this transformation, however, and forsterite may persist metastably to much higher pressures and may be present in subducted lithospheric slabs to depths as great as 660 km (24 GPa) (Sung and Burns 1976; Rubie and Ross 1994).

The need to understand the structure and behavior of the upper mantle and of subducted lithospheric slabs has prompted numerous experimental investigations of the properties of forsterite at high pressure. Experimental X-ray diffraction and vibrational spectroscopy studies have both found evidence for a sudden change in the compressional behavior of forsterite near 9 GPa (Kudoh and Takéuchi 1985; Chopelas 1990). However, the compressional anomalies seen in single-crystal X-ray diffraction experiments have not been reproduced by more recent experiments that used a more hydrostatic pressure medium (Downs et al. 1996). An understanding of these results is essential because rapid changes in compression mechanism have important consequences for the elastic constants, and therefore for the seismic wave velocities of this geophysically important mineral.

In this paper we present a first-principles study of forsterite's behavior under compression at zero temperature. The aim is to elucidate the origin of the anisotropic behavior under pressure and to investigate the nature of the compressional anomaly, if any, at the atomic scale.

COMPUTATIONAL METHOD

We use the plane-wave pseudopotential method (e.g., Cohen and Chelikowsky 1988) to solve the equations of density functional theory (Kohn and Sham 1965) in the local density approximation (LDA). An important issue in computations of complex structures, such as that of forsterite, is the efficient determination of the ground state (equilibrium) arrangement of the atoms. To find the equilibrium structure of forsterite at each pressure, we have used a first-principles implementation (Wentzcovitch 1995) of a variable cell-shape molecular dynamics (VCSMD) algorithm (Wentzcovitch 1991). This method has been successfully used to determine the compressive and elastic behavior of other minerals under compression (Wentzcovitch et al. 1995a, 1995b). It is a quite conventional implementation of first principles molecular dynamics (MD) in which forces and stresses are calculated self-consistently (Wentzcovitch and Martins 1991) at every time step by resorting of iterative diagonalization

0003–004X/97/0708–0663$05.00

(Martins et al. 1991) and charge mixing (Broyden 1965) to speed up the convergency process.

The equilibrium structure at arbitrary pressures can be found by performing this dynamics in damped mode and searching efficiently for the atomic configuration with zero stresses and forces (Wentzcovitch et al. 1993). For a structure with 14 degrees of freedom like forsterite, typically it takes 20–30 time steps to determine these parameters with three decimal digits. Care must be taken initially to choose a convenient fictitious cell mass that produces strain oscillations with periods similar to those of the atomic oscillations. The atomic masses can also be freely chosen. Whenever possible it is convenient to set all of them equal so we have a smaller range of frequencies for phonon modes. In the present case this was not the best approach. The Mg-O bonds are substantially more compressible than the Si-O bonds (smaller force constants), therefore Mg ions should be assigned smaller masses. The final choice was $M_{Si} = M_O = 15\ m_p$ and $M_{Mg} = 10\ m_p$ (proton masses), and the fictitious cell mass $W = 0.001\ m_p a_o^{-4}$ (a_o is the Bohr radius). The MD time step is another free parameter in this algorithm, and it is chosen to minimize the number of total steps during the minimization. It is related to the average frequency of normal modes such that it takes 4–10 steps per average period. Ideally it would be desirable to have all normal modes with the same period and about two time steps per period; however, it is difficult to ''guess'' suitable free parameters to produce this situation, and practical experience usually dictates the choice. Note that the final structure does not depend on masses or time steps.

In this particular formulation of VCSMD the initial space group symmetry of the structure (*Pbnm*) is conserved if there are no thermal fluctuations, as it happens in the damped dynamics minimization (Wentzcovitch 1991). This property can be exploited in first-principles calculations by reducing *k*-point sampling to the irreducible wedge of the Brillouin zone (IBZ) and symmetrizing the resulting charge densities, forces, and stresses. Our results were obtained with one *k* point (¼, ¼, ¼) in the IBZ, corresponding to a Monkhorst-Pack grid of 2×2×2. The plane-wave expansion energy cut off (E_{pw}) have been chosen as 70 and 280 Ry for the wave functions and charge density-potentials, respectively (Calc. I). We have used the same Troullier-Martins (1991) pseudopotentials for Si, Mg, and O from previous studies of other silicates of magnesium polymorphs (Wentzcovitch and Price 1996). The convergence of the present results have been tested by performing completely similar calculations at the same *k* point and E_{pw} equal to 64 Ry for wave functions, charge densities, and potential (Calc. II). This second set of calculations provided a comparison of compressibilities and structural parameters. A third series of calculations (Calc. III) using eight *k* points and the same E_{pw} as Calculation I at the lowest pressure provided a better estimate of the accuracy of the zero-pressure parameters.

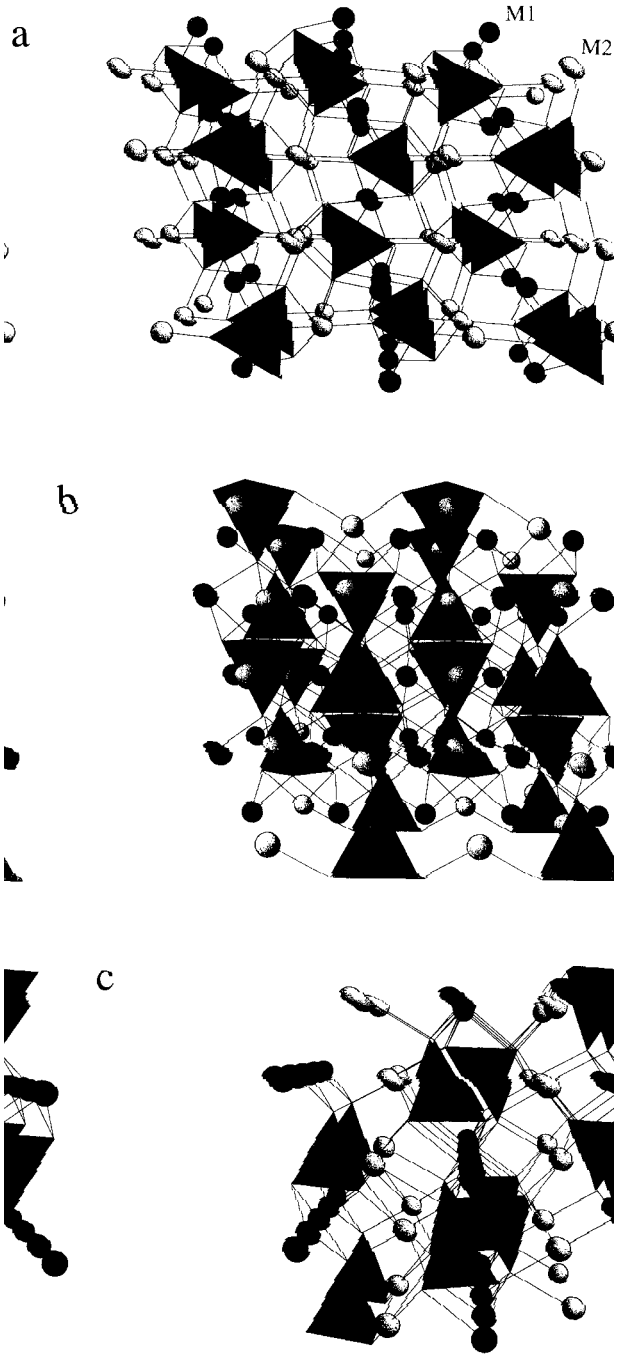

FIGURE 1. Views of the forsterite structure along (**a**) [100], (**b**) [010], and (**c**) [001]. Dark and light circles represent M1 and M2 cations, respectively.

RESULTS

The crystal structure of forsterite is shown in Figure 1 as viewed along the three main crystallographic axes. There are two crystallographically distinct octahedral sites occupied by Mg ions (M1 and M2) represented by spheres of different shades, one tetrahedral site occupied by S, and three distinct O positions (O1, O2, and O3) at

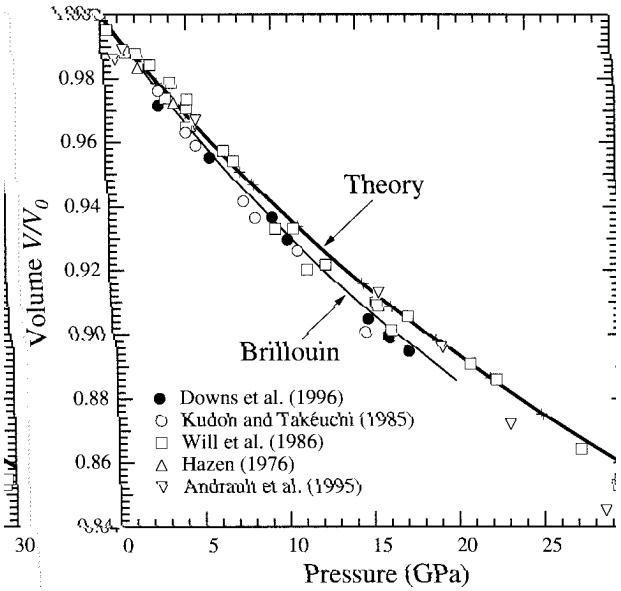

FIGURE 2. Theoretical equation of state (crosses and bold line) compared with the equation of state inferred from the Brillouin measurements (light line) of Zha et al. (1996) and the results of X-ray diffraction experiments as indicated.

tetrahedral corners. The O substructure forms a significantly distorted hexagonal close-packed arrangement because of the presence of non-uniform occupation of interstitial sites by Mg and S. This non-uniform occupation also gives rise to highly anisotropic behavior under compression, which has been the subject of several previous investigations (Hazen 1976; Kudoh and Takéuchi 1985) including one previous first-principles calculation (Brodholt et al. 1996). The origin of this anisotropic behavior has been addressed experimentally mostly by comparative crystal chemistry (Hazen 1976; Kudoh and Takéuchi 1985; Kudoh and Takeda 1986; Sharp et al. 1987; Hazen et al. 1996). Besides anisotropy, another issue related with its behavior under compression has been raised: a possible change in compression mechanism at high pressures, or a second-order phase transition (Kudoh and Takéuchi 1985). The experimental determination of structural parameters that led to the proposed anomalous compressibility was recently questioned by another experimental study that related the anomaly in the X-ray data to the freezing of the hydrostatic medium (4:1 ethanol to methanol mixture or Ar) between 9–10 GPa (Downs et al. 1996). This would also provide a possible explanation for the anomalies observed in Raman and infrared spectroscopic studies at similar pressures (Chopelas 1990; Wang et al. 1993; Durben et al. 1993; Liu and Mernagh 1994).

First-principles calculations provide an independent means to investigate details of the structural behavior under compression at the atomic level. The equation of state obtained in our calculations (Calc. I) is shown in Figure 2. The agreement with experimental data over the pressure range of our study is good. The theoretical zero-pressure lattice parameters are 1.5, 2.3, and 2.3% smaller for *a*, *b*, and *c*, respectively, than the experimental values (see Table 1).

This difference is due to the fundamental approximation (LDA) upon which our calculations are based (Lundqvist and March 1987). The theoretical equation of state yields a compressibility slightly less than the experimental one. The zero-pressure bulk modulus obtained by fitting a third-order Birch-Murnaghan finite-strain expansion to our theoretical results is 135 GPa ($K_0' = 4.9$), 6%

TABLE 1. Computed structural parameters at different pressures (Calc. I unless otherwise noted)

P				Si		Mg2		O1		O2		O3		
(GPa)	*a* (Å)	*b* (Å)	*c* (Å)	*x*	*y*	*x*	*y*	*x*	*y*	*x*	*y*	*x*	*y*	*z*
0	4.682	9.953	5.837	0.4227	0.0938	0.9913	0.2756	0.7719	0.0913	0.2238	0.4438	0.2731	0.1639	0.0287
0*	4.649	9.971	5.846	0.4279	0.0953	0.9915	0.2759	0.7736	0.0923	0.2218	0.4448	0.2722	0.1662	0.0296
0†	4.678	9.952	5.840	0.4270	0.0931	0.9909	0.2749	0.7710	0.0907	0.2243	0.4429	0.2726	0.1638	0.0281
Exp‡	4.750	10.187	5.977	0.4276	0.0941	0.9916	0.2775	0.766	0.0914	0.2215	0.4472	0.2778	0.1631	0.0332
HCP§				5/12	1/12	3/4	1/12	3/4	1/12	1/4	1/12	1/4	1/6	0.0
3.1	4.660	9.858	5.794	0.4275	0.0941	0.9907	0.2753	0.7723	0.0913	0.2244	0.4430	0.2718	0.1645	0.0279
4.7	4.649	9.818	5.775	0.4275	0.0942	0.9904	0.2751	0.7725	0.0913	0.2244	0.4426	0.2711	0.1648	0.0273
5.3	4.646	9.804	5.765	0.4276	0.0943	0.9904	0.2750	0.7726	0.0913	0.2244	0.4425	0.2708	0.1649	0.0271
7.9	4.630	9.738	5.734	0.4275	0.0945	0.9901	0.2747	0.7729	0.0913	0.2247	0.4419	0.2698	0.1653	0.0264
8.6	4.626	9.722	5.725	0.4275	0.0945	0.9900	0.2746	0.7729	0.0913	0.2248	0.4418	0.2696	0.1655	0.0263
11.1	4.613	9.665	5.697	0.4275	0.0945	0.9900	0.2746	0.7729	0.0913	0.2251	0.4413	0.2687	0.1658	0.0257
14.9	4.593	9.586	5.658	0.4274	0.0950	0.9894	0.2741	0.7735	0.0911	0.2254	0.4407	0.2674	0.1664	0.0248
16.5	4.585	9.553	5.642	0.4274	0.0951	0.9892	0.2740	0.7736	0.0911	0.2256	0.4404	0.2669	0.1666	0.0245
19.0	4.574	9.505	5.619	0.4274	0.0951	0.9889	0.2739	0.7736	0.0910	0.2260	0.4400	0.2660	0.167	0.0245
22.0	4.561	9.452	5.592	0.4272	0.0955	0.9887	0.2737	0.7737	0.0908	0.2263	0.4396	0.2650	0.1673	0.0234
25.0	4.547	9.402	5.567	0.4275	0.0955	0.9892	0.2733	0.7741	0.0906	0.2263	0.4392	0.2643	0.1677	0.0231

Note: Atomic coordinates: Mg1: (0, 0, 0), (0, 0, ½), (½, ½, 0), and (½, ½, ½). Mg2: ±(Mg2$_x$, Mg2$_y$, ¼; Mg2$_x$ + ½, ½ − Mg2$_y$, ¾). Si: ±(Si$_x$, Si$_y$, ¼; Si$_x$ + ½, ½ − Si$_y$, ¾). O1: ±(O1$_x$, O1$_y$, ¼; O1$_x$ + ½, ½ − O1$_y$, ¼). O2: ±(O2$_x$, O2$_y$ ¼; O2$_x$ + ½, ½ − O2$_y$, ¼). O3: ±(O3$_x$, O3$_y$, O3$_z$; O3$_x$, O3$_y$, ½ − O3$_z$; O3$_x$ + ½, ½ − O3$_y$, −O3$_z$; ½ + O3$_x$, ½ − O3$_y$, ½ + O3$_z$).

* Calculation II.

† Calculation III.

‡ Kudoh and Takeʹuchi (1985).

§ Ideal hcp structure.

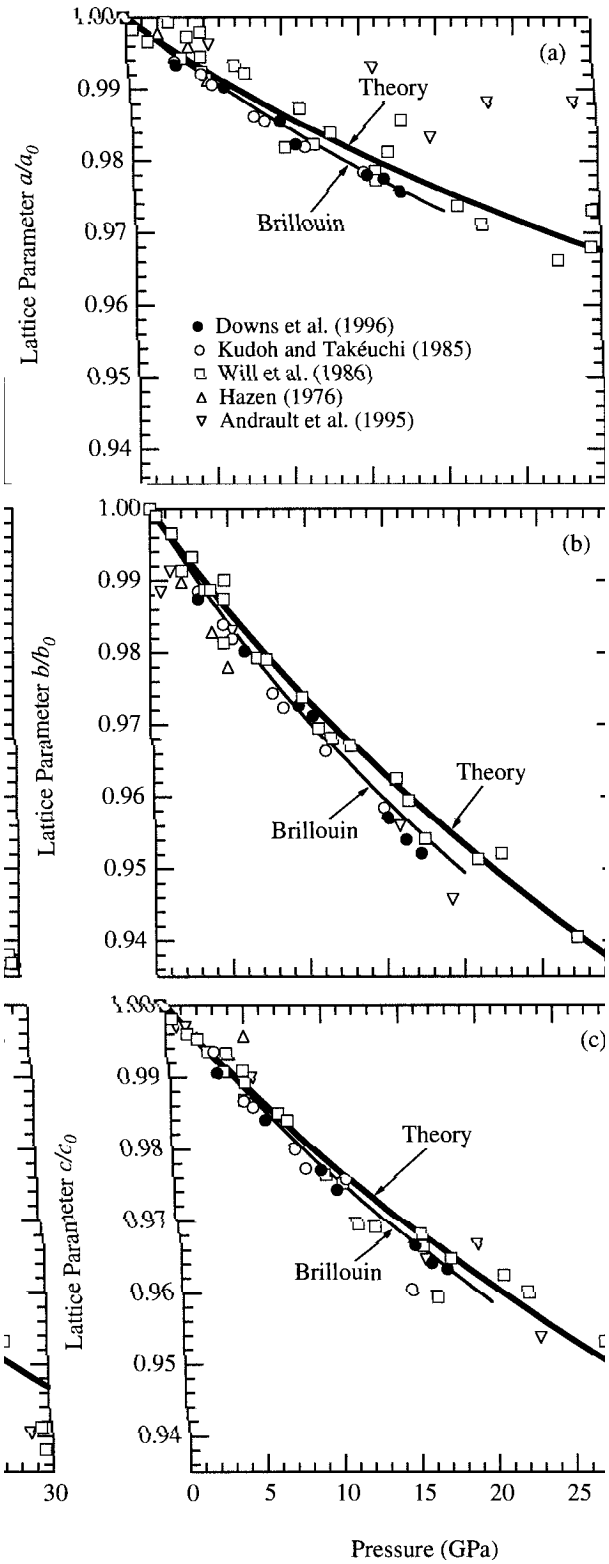

FIGURE 3. Lattice parameters as a function of pressure (bold lines) compared with those inferred from the Brillouin measurements (light lines) of Zha et al. (1996) and the results of X-ray diffraction experiments as indicated.

larger than the experimental value of 127 GPa (Zha et al. 1996).

The pressure dependence of the lattice parameters obtained theoretically also agrees well with experiment: We find that the *a* axis compresses the least, while the *b* axis is most compressible, as observed experimentally (Fig. 3, Table 1). We compare our results with X-ray diffraction experiments and with recent determinations of the elastic constants of forsterite to 16 GPa (Zha et al. 1996). We obtain the pressure dependence of the lattice parameters implied by the elastic constant measurements by integrating

$$\alpha(P)/\alpha_0 = \exp\left[-\int_0^P K_\alpha(P')\mathrm{d}P'\right] \tag{1}$$

where $\alpha = a$, b, and c, the lattice parameters at pressure P are $\alpha(P)$, and α_0 are the lattice parameters at zero pressure. The linear bulk moduli are defined by $K_\alpha = (\partial P/\partial \ln\alpha)T$ and are given in terms of the measured elastic constants, C_{ij}, by (Nye 1985)

$$K_a = \frac{D}{(C_{33}-C_{13})(C_{22}-C_{12})-(C_{23}-C_{12})(C_{23}-C_{13})} \tag{2}$$

$$K_b = \frac{D}{(C_{33}-C_{23})(C_{11}-C_{12})-(C_{13}-C_{12})(C_{13}-C_{23})} \tag{3}$$

$$K_c = \frac{D}{(C_{22}-C_{23})(C_{11}-C_{13})-(C_{12}-C_{13})(C_{12}-C_{23})} \tag{4}$$

$$D = C_{11}C_{22}C_{33} + 2C_{12}C_{13}C_{23} - C_{11}C_{23}^2 - C_{22}C_{13}^2 - C_{33}C_{12}^2. \tag{5}$$

Our theoretical values of α/α_0 agree within 0.3% with those experimentally inferred from elastic constant measurements and with the results of most previous X-ray diffraction measurements (Fig. 3). The agreement between theory and the X-ray diffraction results of Will et al. (1986) and Andrault et al. (1995) is significantly worse, possibly due to non-hydrostaticity in these experiments.

Our theoretical results confirm the anisotropic compression of olivine seen experimentally and show that this anisotropy persists throughout its stability field. To show this, we determined the linear bulk moduli from our theoretical calculations by fitting our determinations of the lattice parameters as a function of pressure to linear finite-strain expansions (Davies 1974; Weaver 1976; Meade and Jeanloz 1990)

$$F_\alpha = K_\alpha + m_\alpha f_\alpha \tag{6}$$

where f_α is the Eulerian finite strain

$$f_\alpha = \frac{1}{2}\left[\left(\frac{\alpha}{\alpha_0}\right)^2 - 1\right] \tag{7}$$

$$F_\alpha = \frac{P}{f_\alpha(1+2f_\alpha)(1+2f_v)} \tag{8}$$

f_v is the volume Eulerian finite strain

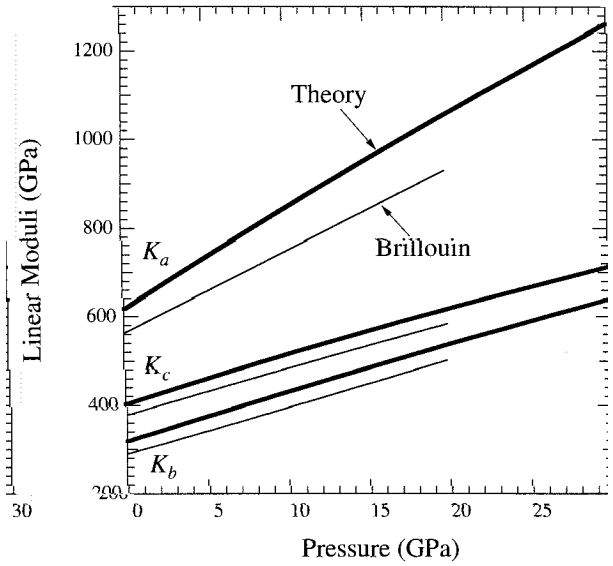

FIGURE 4. Linear moduli as a function of pressure. Theoretical results are shown as bold lines, and the results of Zha et al. (1996) as light lines. For a material that compresses isotropically, the linear modulus is three times the bulk modulus.

$$f_v = \frac{1}{2}\left[\left(\frac{V_0}{V}\right)^{-2/3} - 1\right] \tag{9}$$

and m_α is related to the pressure dependence of K_α. The results are compared with the linear moduli as determined from the measured elastic constants (Zha et al. 1996) through Equations 2–5. Figure 4 shows that the theoretical linear moduli are larger than those experimentally measured by 13% at most. Both theory and experiment show that the compressional anisotropy persists to at least 25 GPa. The magnitude of the anisotropy changes little with pressure over the range investigated: The ratio K_a/K_b changes from 1.93 at 0 GPa to 1.97 at 25 GPa. The change in K_a/K_c is more substantial: from 1.53 at 0 GPa to 1.74 at 25 GPa.

The dependence of the volume and lattice parameters on pressure (Figs. 2 and 3) is smooth and shows no rapid changes in slope over the pressure range investigated. These results support the conclusions of Brodholt et al. (1996), based on their pseudopotential calculations, that no rapid change in bulk or linear compressibility occurs in olivine over the pressure range 0–25 GPa. The smooth variation of lattice parameters with pressure found here does not support the conclusions of Kudoh and Takéuchi (1985) that there is a change in the linear and volume compressibilites of forsterite near 9 GPa. Previous studies suggested that more subtle pressure-induced changes in compression may exist. A change in compression mechanism might not necessarily be reflected in the equation of state or linear compressibilites. Chopelas (1990), Wang et al. (1993), and Durben et al. (1993) found anomalous pressure dependencies of vibrational modes, which may be caused by such a change in compression mechanism. An examination of pressure-induced changes in internal structural parameters allows us to test this picture.

The SiO_4 tetrahedron in forsterite has three unique bond lengths. Theoretically predicted Si-O bond lengths are within 0.3% of experimental values at zero pressure (Fig. 5). In agreement with the experimental zero-pressure structure, we find that Si-O2 is the longest, Si-O1 is the shortest, and that these differ by 2.5%. Predicted bond lengths in the M1 and M2 octahedra are somewhat smaller than experimentally observed (by 2.5%). This discrepancy, also found by Brodholt et al. (1996) and in LDA calculations of enstatite (Wentzcovitch et al. 1995b), accounts for the smaller zero-pressure volume and larger bulk modulus of our theoretical results compared with experiment. Its origin is most likely related to the use of the LDA. As a result, our calculations find the correct ordering and dispersion of Mg-O bond lengths: In the M1 octahedron, M1-O3 (longest) and M1-O2 $\approx$ M1-O1 (shortest) differ by 3%; whereas in the M2 octahedron, M2-O3 (longest) and M2-O2 (shortest) differ by 7%. This is important because the relative lengths of bonds are expected to control compressional anisotropy and compression mechanisms.

We find that SiO_4 and MgO_6 polyhedra compress nearly isotropically (Fig. 5). The ordering of Si-O bond lengths remains unchanged up to 25 GPa, while the difference between longest and shortest increases only slightly with compression. Except for an increase in the difference between Mg1-O1 and Mg1-O2 bond lengths, the ordering of Mg-O bond lengths is also unchanged by compression. The nearly isotropic compression of the coordination polyhedra can also be characterized by the quadratic elongation (Robinson et al. 1971). We find that the Mg octahedra become slightly more ideal (smaller quadratic elongation) with increasing pressure, whereas the tetrahedron becomes slightly more distorted (larger quadratic elongation) with increasing pressure. The pressure-induced changes in quadratic elongations are small: Elongations of the Si, M1, and M2 polyhedra change by 0.3, 0.6, and 0.6%, respectively, between 0 and 25 GPa. Although these are significant differences in terms of the precision of our calculations, they are small compared with the decrease in bond lengths experienced by these polyhedra over the same pressure range.

Our calculations show that the SiO_4 polyhedra compress much less than the Mg polyhedra, as expected on the basis of the greater strength of the Si-O bond and experimental studies of other silicates (Hazen and Finger 1982). The total change in volume of the Si, M1, and M2 polyhedra between 0 and 25 GPa is 6, 13, and 16%, respectively. The zero-pressure polyhedral bulk moduli (Hazen and Finger 1979) span the bulk modulus of the crystal (Table 2).

The theoretical calculations show important similarities to the high-pressure crystal structure refinements of Kudoh and Takéuchi (1985). Though the scatter in the data is substantial, the tendency of the polyhedra to compress approximately isotropically is evident in some cases (Fig.

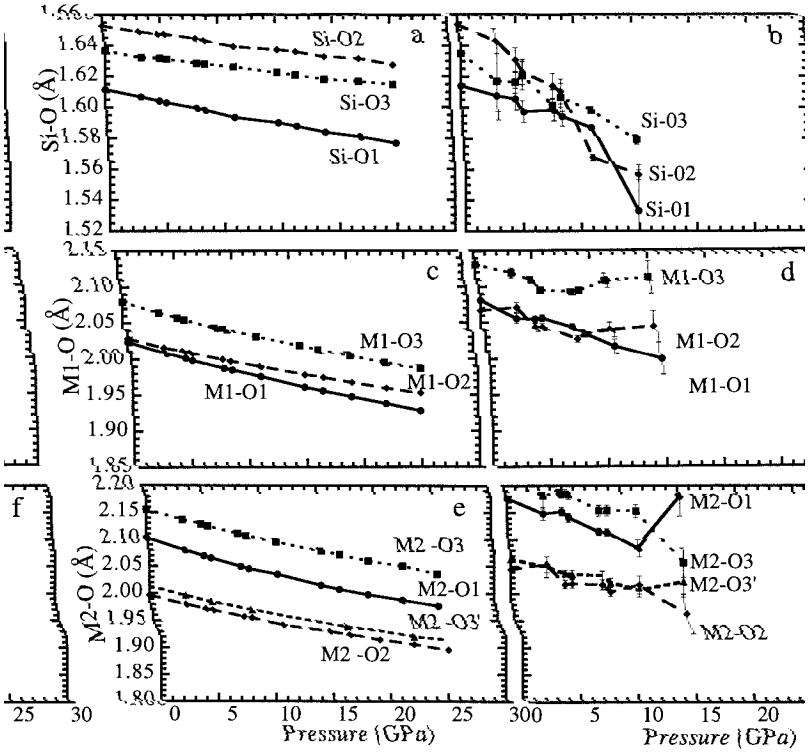

FIGURE 5. Internal bond lengths of various polyhedra vs. pressure. (**a**) and (**b**) correspond to SiO_4 tetrahedra, (**c**) and (**d**) to $Mg1O_6$ octahedra, and (**e**) and (**f**) to $Mg2O_6$ octahedra. (**a**), (**c**), and (**e**) correspond to our results and (**b**), (**d**), and (**f**) correspond to Kudoh and Takéuchi's (1985) results.

5). As in our calculations, M1-O1 remains the shortest bond in the M1 octahedron, and M1-O3 the longest over the experimental pressure range (Fig. 5). In the M2 octahedron, except for the highest experimental refinement, where uncertainties are substantial, the M2-O3 bond remains the longest, and M2-O2 the shortest. In the Si tetrahedron, Si-O3 remains longer than Si-O1, but Si-O2 compresses much more in the experiments than in our calculations.

There are also significant differences between experiment and theory. The experimental data show that the SiO_4 tetrahedron is as compressible as the Mg octahedra, in disagreement with our results and with the behavior of essentially all other high-pressure silicate crystal structure refinements (Fig. 6). In comparison with our results, the

TABLE 2. Crystal and polyhedral bulk moduli

		Calc. I	Calc. II	Exp.
Forsterite	K_0	135	134	123*
				120†
	K_0'	4.9	5.5	5.6*
SiO_4	K_0	407	367	190*
				550‡
$M1O_6$	K_0	158	181	140*
				120‡
$M2O_6$	K_0	118	128	130*
				100‡

Note: Polyhedral bulk moduli obtained from second-order Eulerian finite-strain fits ($K_0' = 4.0$); third-order fits were not significantly better.
* Kudoh and Takéuchi (1985).
† Olinger (1977).
‡ Hazen (1976).

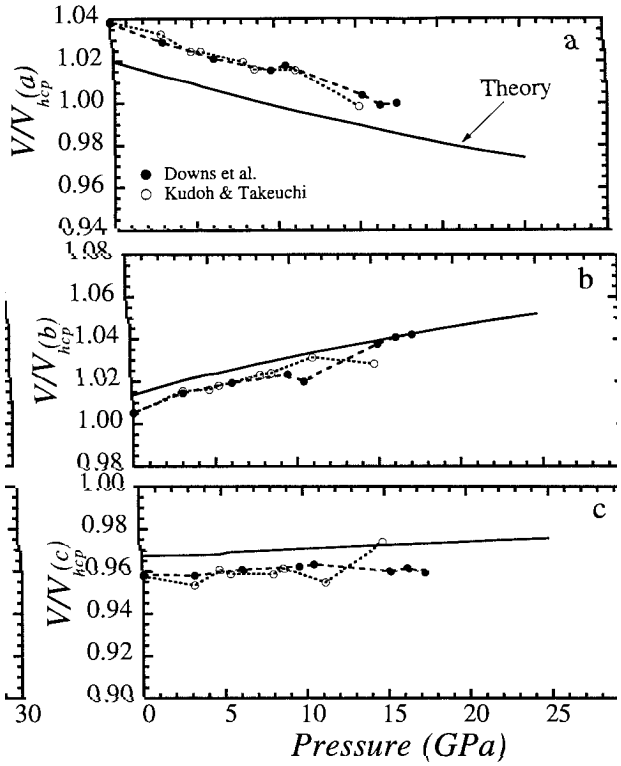

FIGURE 6. Polyhedral volumes vs. pressure. Open circles with error bars were obtained from parameters given by Kudoh and Takéuchi (1985). Our calculated results are given by full circles.

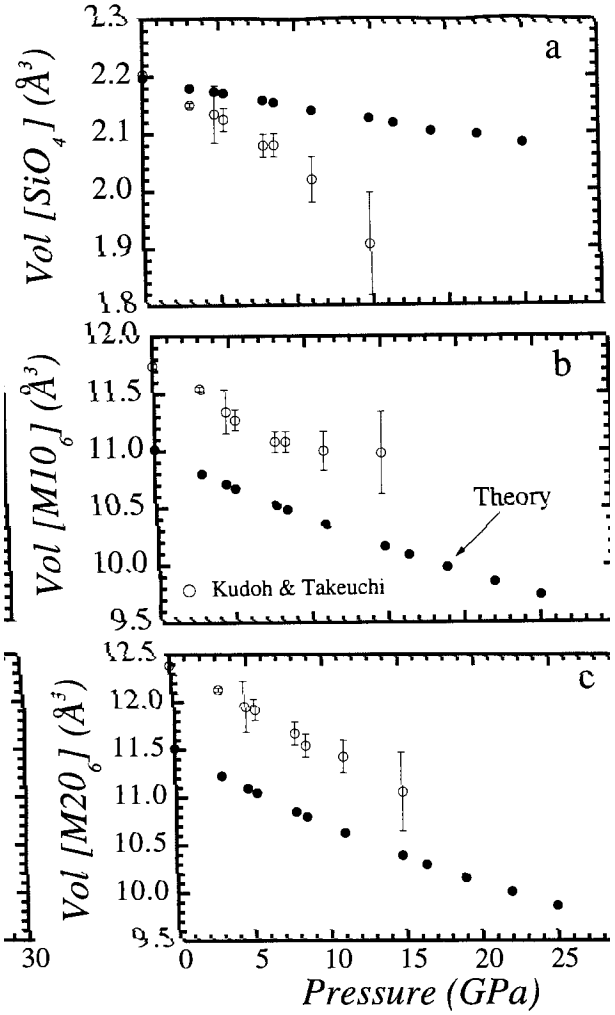

FIGURE 7. Pressure dependence of the ratios of real cell volume, V, to ideal calculated cell volume, V_{hcp}, for three arbitrary definitions of V_{hcp} in terms of lattice parameters a, b, and c. See text.

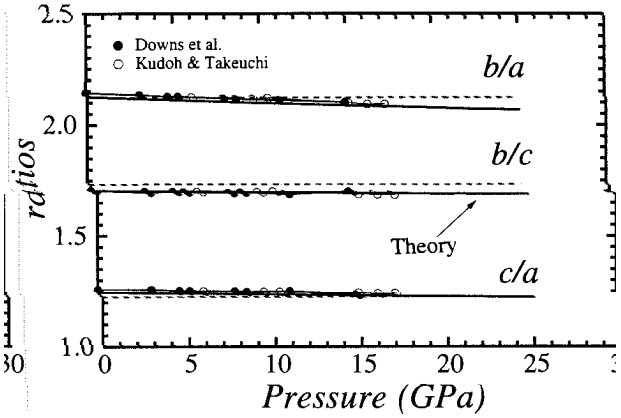

FIGURE 8. Pressure dependence of the axial ratios. The dashed lines correspond to the ideal ratios in the hcp structure. Open circles are data from Kudoh and Takéuchi (1985), and full circles are from Downs et al. (1996). See text.

experimental data exhibit much more anisotropic and irregular compression of the polyhedra as shown by the measured polyhedral elongations as a function of pressure. Kudoh and Takéuchi found that M1-O3, M1-O2, M2-O1, and M2-O3′ increase with pressure in disagreement with our results and with experimental data for other minerals. This pressure-induced increase in Mg-O bond lengths is reflected in a sudden change in the compressibility of the M1 octahedron near 9 GPa. This result is inconsistent with our theoretical calculations. We find no evidence in the pressure dependence of bond lengths and polyhedral volumes for a sudden change in compressibility of any structural element between 0 and 25 GPa. Our theoretical results support those of Brodholt et al. (1996) who analyzed variations in internal structural parameters only in terms of average bond lengths.

Another issue raised by Kudoh and Takéuchi's analysis of their data concerns the distortion of the O substructure. The compressibility of the M1 octahedron decreases, and at 16.5 GPa its volume becomes nearly equal to that of the larger M2 octahedron. They noted that at this pressure the primitive cell volume, V_{obs}, tends to that corresponding to an ideal hexagonal close-packed structure V_{hcp}. For the ideal lattice the axial ratios a:b:c are expected to be $1:\sqrt{3}/\sqrt{2}:\sqrt{3}/2$, with a perpendicular to the O layers, and the volume would be given by $V_{hcp}(a) = 3\sqrt{3}a^3/2$. We note that V_{hcp} could also be expressed in term of b and c as $V_{hcp}(b) = \sqrt{2}/3\sqrt{3}b^3$ and $V_{hcp}(c) = \sqrt{2}c^3$. Therefore the choice of a is arbitrary and this is shown in Figure 7, where the pressure dependences of the volume ratios, V_{obs}/V_{hcp}, for the three arbitrary choices are plotted. Although V_{obs}/V_{hcp} (a) approaches 1.0 under pressure, V_{obs}/V_{hcp} (b) departs from 1.0, so it is incorrect to conclude that the structure becomes less distorted under pressure. Indeed, if we compare the pressure dependence of the axial ratios, as is done in Figure 8, we arrive at the opposite conclusion: Only c/a approaches the ideal value $\sqrt{3}/2$, the other ratios, b/a and b/c, depart from their respective values (dashed lines in Fig. 8).

DISCUSSION

We find no anomalies in the compression of forsterite to a pressure of 25 GPa. The volume and lattice parameters show no sudden changes in their compressibilites. Moreover, bond lengths and polyhedral volumes also decrease smoothly with pressure. We therefore find that no obvious changes occur in compression mechanism over the pressure range studied. These results are inconsistent with the existence of sudden changes in the compressibility of lattice parameters or bond lengths (Kudoh and Takéuchi 1985) or with sudden changes in mode Grüneisen parameters (Chopelas 1990) and support the results of Brodholt et al. (1996). The theoretical calculations lend support to the conclusions of Downs et al. (1996) that previous evidence for compressional anomalies in forsterite are due to the sudden onset of non-hydrostaticity

in the experiments, which is known to occur at approximately the same pressure at which the compressional anomalies were seen (9 GPa).

The compression of forsterite is found to be significantly anisotropic up to at least 25 GPa. The *b* axis is nearly twice as compressible as the *a* axis over the entire pressure range. The compressional anisotropy of olivine is only weakly dependent on pressure. This result is of seismological as well as crystal-chemical interest. The anisotropy of olivine plays a central role in the interpretation of seismological measurements of the radial and transverse anisotropy of the upper mantle (Tanimoto and Anderson 1984). We note however, that our theoretical results provide only a partial description of P- and S-wave anisotropies in this mineral, constraining only the three combinations of elastic constants (Eq. 2–5). A complete theoretical description of the anisotropy of forsterite and its pressure dependence awaits a theoretical determination of the full elastic constant tensor.

Despite the strongly anisotropic compression of the forsterite structure, we find that the coordination polyhedra compress nearly isotropically. This seeming contradiction is resolved by recognizing that the forsterite structure is inherently anisotropic, with rows of relatively compressible (Mg1 octahedra) and incompressible (Si tetrahedra) polyhedra alternating along [100] (Hazen 1987). To illustrate this, we show that the relative magnitudes of K_a, K_b, and K_c can be rationalized in terms of polyhedral compressibilities. We assume that the polyhedra compress perfectly isotropically and that they suffer no rotation under compression. A consideration of the elements of the forsterite structure then allows us to relate directly polyhedral and axial compressibilities. Parallel to [001] are chains of edge-sharing M1 octahedra. These chains of M1 octahedra alternate along the [010] axis with M2 octahedra. Along the [100] axis, the M1 octahedral chains alternate with rows of Si tetrahedra. Remembering that linear and volume compressibilities are related by a factor of three, and using the polyhedral moduli from our LDA results, the axial compressibilities can be approximated by

$$K_a \approx 6(1/K_{\mathrm{Mg1}} + 1/K_{\mathrm{Si}})^{-1} = 683 \text{ GPa} \quad (10)$$

$$K_b \approx 6(1/K_{\mathrm{Mg1}} + 1/K_{\mathrm{Mg2}})^{-1} = 405 \text{ GPa} \quad (11)$$

$$K_c \approx 3K_{\mathrm{Mg1}} = 474 \text{ GPa}. \quad (12)$$

The axial moduli predicted by this simple structural model are all significantly overestimated in comparison with the results of our quantum mechanical calculations (Fig. 4). The reason for this is that the structural model is oversimplified. If we take into account polyhedral distortions and the rotation of octahedra, for instance rotations of the M1 octahedra about their shared edges, the predicted moduli are smaller and in better agreement with our LDA results. However, the relative magnitudes of the axial moduli are correct ($K_a > K_b > K_c$) and the ratios of the moduli ($K_a/K_b = 1.68$, $K_a/K_c = 1.46$) are similar to those derived from the LDA results. This shows that the anisotropic compression of the forsterite structure can be explained essentially in terms of isotropic polyhedral compressibilities. Hazen (1987) came to a similar conclusion. However, he assumed that $K_{\mathrm{Mg1}} \approx K_{\mathrm{Mg2}}$ and restricted his analysis to the ratio K_a/K_b. He further assumed, as we have done, that the polyhedra compress approximately isotropically. Our LDA calculations, which show that pressure-induced changes in quadratic elongation are small, lend substantial theoretical support to this assumption. This prediction must be tested against new high-resolution crystal-structure refinements at high pressure.

Acknowledgments

We thank K. Refson and an anonymous reviewer for helpful comments on the manuscript. R.M.W. thanks Robert Downs for providing the program XTALDRAW for structural analysis. This work was supported by the National Science Foundation under grants EAR-9628042 (R.M.W.) and EAR-9628199 (L.P.S.), and by the Minnesota Supercomputer Institute.

References cited

Andrault, D., Bouhifd, M.A., Itie, J.P., and Richet, P. (1995) Compression and amorphization of $(Mg,Fe)_2SiO_4$ olivines: an x-ray diffraction study up to 70 GPa. Physics and Chemistry of Minerals, 22, 99–107.

Brodholt, J., Patel, A., and Refson, K. (1996) An ab initio study of the compressional behavior of forsterite. American Mineralogist, 81, 257–260.

Broyden, C.G. (1965) A class of methods for solving nonlinear simultaneous equations. Mathematical Computation, 19, 577–593.

Chopelas, A. (1990) Thermal properties of forsterite at mantle pressures derived from vibrational spectroscopy. Physics and Chemistry of Minerals, 17, 149–156.

Cohen, M.L. and Chelikowsky, J.R. (1988) Electronic structure and optical properties of semiconductors. Springer-Verlag, New York.

Davies, G.F. (1974) Effective elastic moduli under hydrostatic stress—I. quasiharmonic theory. Journal of the Physics and Chemistry of Solids, 35, 1513–1520.

Downs, R.T., Zha, C.-S., Duffy, T.S., and Finger, L. (1996) The equation of state of forsterite to 17.2 GPa and effects of pressure media. American Mineralogist, 81, 51–55.

Durben, D.J., McMillan, P.F., and Wolf, G.H. (1993) Raman study of the high-pressure behavior of forsterite (Mg_2SiO_4) crystal and glass. American Mineralogist, 78, 1143–1148.

Hazen, R.M. (1976) Effects of temperature and pressure on the crystal structure of forsterite. American Mineralogist, 61, 1280–1293.

——(1987) High pressure crystal chemistry of Chrysoberyl, Al_2BeO_4: insights on the origin of elastic anisotropy. Physics and Chemistry of Minerals, 14,13–20.

Hazen, R.M. and Finger, L.W. (1979) Bulk-modulus volume relationship for cation-anion polyhedra. Journal of Geophysical Research, 84, 6723–6728.

——(1982) Comparative Crystal Chemistry, 231 p. Wiley, New York.

Hazen, R.M., Downs, R.T., and Finger, L.W. (1996) High-pressure crystal chemistry of $LiScSiO_4$: An olivine with nearly isotropic compression. American Mineralogist, 81, 327–334.

Liu, L.G. and Mernagh, T.P. (1994) Raman spectra of forsterite and fayalite at high pressures and room temperature. High Pressure Research, 11, 241–256.

Kohn, W. and Sham, L.J. (1965) Self-consistent equations including exchange and correlation effects. Physical Review, 140, A1133-A1138.

Kudoh, Y. and Takeda, H. (1986) Single crystal x-ray diffraction study on the bond compressibility of fayalite, Fe_2SiO_4 and rutile, TiO_2 under high pressure. Physica, 139 and 140B, 333–336.

Kudoh, Y. and Takéuchi, Y. (1985) The crystal structure of forsterite Mg_2SiO_4 under high pressure up to 149 kbar. Zeitschrift für Kristallographie, 171, 291–302.

Lundqvist, S. and March, N.H. (1987) Theory of the inhomogeneous electron gas. Plenum Press, London.

Martins, J.L., Troullier, N., and Wei, S. (1991) Plane-wave pseudopotential calculation for ZnS. Physical Review B, 43, 2213–2217.

Meade, C. and Jeanloz, R. (1990) Static compression of $Ca(OH)_2$ at room temperature: observations of amorphization and equation of state measurements to 10.7 GPa. Geophysical Research Letters, 17, 1157–1160.

Nye, J.F. (1985) Physical properties of crystals. Oxford University Press, Oxford, U.K.

Robinson, K., Gibbs, G.V., and Ribbe, P.H. (1971) Quadratic elongation: a quantitative measure of distortion in coordination polyhedra. Science, 172, 567–570.

Rubie, D.C. and Ross, C.R. (1994) Kinetics of the olivine-spinel transformation in subducting lithosphere—experimental constraints and implications for deep slab processes. Physics of the Earth and Planetary Interiors, 86, 223–241.

Sharp, Z.D., Hazen, R.M., and Finger, L.W. (1987) High-pressure crystal chemistry of monticellite, $CaMgSiO_4$. American Mineralogist, 72, 748–755.

Sung, C.M. and Burns, R.G. (1976) Kinetics of the olivine-spinel transition: implications for deep-focus earthquake genesis. Earth and Planetary Science Letters, 23, 165–170.

Tanimoto, T. and Anderson, D.L. (1984) Mapping convection in the mantle. Geophysical Research Letters, 11, 287–290.

Troullier, N. and Martins, J.L. (1991) Efficient pseudopotentials for plane-wave calculations. Physical Review B, 43, 1993–2003.

Wang, S.Y., Sharma, S.K., and Cooney, T.F. (1993) Micro-Raman and infrared spectral study of forsterite under high pressure. American Mineralogist, 78, 469–476.

Weaver, J.S. (1976) Application of finite strain theory to non-cubic crystals. Journal of the Physics and Chemistry of Solids, 37, 711–718.

Wentzcovitch, R.M. (1991) Invariant molecular dynamics approach to structural phase transitions. Physical Review B, 44, 2358–2361.

———(1995) First principles molecular dynamics with variable cell shape. In J. R. Chelikowsky and S. G. Louie, Eds., Quantum mechanical theory of real materials, p. 113-127. Kluwer Academic Publishers, Dordrecht.

Wentzcovitch, R.M. and Martins, J.L. (1991) First principles molecular dynamics of Li: test of a new algorithm. Solid State Communications, 78, 831–834.

Wentzcovitch, R.M. and Price, G.D. (1996) High pressure studies of mantle minerals by ab initio molecular dynamics. In B. Silvi and P. D'Arco, Eds., Modeling of minerals and silicate materials, p. 39–61. Kluwer Academic Publishers, Dordrecht.

Wentzcovitch, R.M., Martins, J.L., and Price, G.D. (1993) Ab initio molecular dynamics with variable cell shape—application to $MgSiO_3$. Physical Review Letters, 70, 3947–3950.

Wentzcovitch, R.M., N.L. Ross, and G.D. Price (1995a) Ab Initio study of $MgSiO_3$ and $CaSiO_3$ perovskites at lower-mantle pressures. Physics of the Earth and Planetary Interiors, 90, 101–112.

Wentzcovitch, R.M., Hugh-Jones, D.A., Angel, R.J., and Price, G.D. (1995b) Ab Initio study of $MgSiO_3$ *C*2/*c* enstatite. Physics and Chemistry of Minerals, 22, 453–460.

Will, G., Hoffbauer, W., Hinze, E., and Lauterjung, J. (1986) The compressibility of forsterite up to 300 kbar measured with synchrotron radiation. Physica, 139 and 140B, 193–197.

Zha, C.-S., Duffy, T., Downs, R.T., Mao, H.-K., and Hemley, R.J. (1996) Sound velocity and elasticity of single-crystal forsterite to 16 GPa. Journal of Geophysical Research, 101, 17535–17545.

Manuscript received September 4, 1996
Manuscript accepted April 2, 1997